SLAC-PUB-530
December 1968
(EXPI)

THE SLAC MONOCHROMATIC PHOTON BEAM*

J. Ballam, G. B. Chadwick, Z. G. T. Guiragossian,
A. Kilert, R. R. Larsen, D. W. G. S. Leith

Stanford Linear Accelerator Center
Stanford University, Stanford, California

and

S. H. Williams

University of California, Lawrence Radiation Laboratory
Berkeley, California

(Submitted to Phys. Rev.)

*Work supported by the U. S. Atomic Energy Commission.

I. INTRODUCTION

The study of high energy photon-nucleon interactions has been hampered by the lack of a source of monochromatic gamma rays. The usual source is a beam of electron Bremsstrahlung radiation with the familiar continuous energy spectrum weighted by k^{-1}, where k is the photon energy. Thus, no a priori photon energy information is available, and the kinematic analysis of reactions has one less constraint than is the usual case for charged beams.

Subtraction experiments, in which the primary electron energy is varied, give the effect of a single energy band, but require enormous statistics, and are appropriate only for the simplest reactions. In all cases the heavy weighting of the Bremsstrahlung spectrum at low energies provides a serious background which limits the useful high energy flux. Bubble chamber exposures to a Bremsstrahlung beam provide analysis of reactions in which all final particles are charged. Narrow resonances, such as the ω^0, whose final state contain at most a single neutral particle can also be observed. Knowledge of the primary energy would allow detection of broader resonances in the reactions involving production of a neutral particle.

A high energy photon beam which utilizes the radiation from the in-flight two-photon annihilation of positrons is now in operation at SLAC. A multi-BeV analyzed positron beam from the linac is directed onto a liquid hydrogen target. The energy spectrum of the photons emanating at a small angle ($\approx$10 mr.) relative to the incident positrons contains a component from the normal Bremsstrahlung process and a monochromatic component arising from the two-body final state of positron annihilation. Although the total Bremsstrahlung cross section is orders of magnitude greater than the total annihilation cross section, the angular intensity of the Bremsstrahlung decreases with increasing angle much more rapidly than

does that of the annihilation radiation and at an angle of several milliradians the contribution to the intensity of the monochromatic component is comparable to that of the integral of the Bremsstrahlung from ~1 BeV to the maximum energy.

This beam is being used for bubble and spark chamber exposures to photons of energies between 4 and 9 GeV, and is capable of producing beams down to about 1 GeV if required.

Beam design considerations are summarized in Section II; the experimental arrangement is described in Section III; Section IV contains the results of the initial tuning of the beam and Section V describes the use of the beam in high energy photoproduction experiments at SLAC.

II. BEAM DESIGN CONSIDERATIONS

A positron beam can produce photons via the processes:

$$e^+ + e^- \longrightarrow 2\gamma \qquad (1)$$

$$e^+ + e^- \longrightarrow 3\gamma \qquad (2)$$

$$e^+ + e^- \longrightarrow e^+ + e^- + \gamma \qquad (3)$$

$$e^+ + Z \longrightarrow e^+ + Z + \gamma \qquad (4)$$

Reactions (2) - (4) constitute an unavoidable background source to the monochromatic photons arising from the two-body final state (1). The relative background from (2) and (3) is independent of the target material while (4) will scale as Z^2. For this reason it is desirable to use hydrogen as the target material.

When a positron of energy E annihilates the energy K of the photon emitted at a laboratory angle (θ) is given to excellent approximation by

$$K = \frac{E}{1 + \frac{E}{M}\frac{\theta^2}{2}} , \qquad (5)$$

where M = 0.51 MeV is the electron mass and $E \gg M$. The symmetric annihilation occurs at an angle $\theta_s = \sqrt{\frac{2M}{E}}$; for a representative positron energy of 10 BeV the symmetric photon is then emitted with an energy of 5 BeV at an angle of 10 mr. From (5) one can see that the contributions to the energy spread ΔK of the monochromatic component due to an incident energy spread of ΔE and a finite angular resolution, $\Delta\theta$, are

$$\left.\frac{\Delta K}{K}\right)_E = 2\,\frac{E-K}{E}\,\frac{\Delta\theta}{\theta} \simeq \frac{\Delta\theta}{\theta} \tag{6}$$

and

$$\left.\frac{\Delta K}{K}\right)_\theta = \frac{K}{E}\,\frac{\Delta E}{E} \simeq \frac{1}{2}\,\frac{\Delta E}{E} \tag{7}$$

where the approximation is for the case $\theta = \theta_s$, the best angle to use on the basis of background considerations. A $\frac{\Delta E}{E}$ of less than 1% is easily attainable at SLAC. The net angular acceptance $\Delta\theta$ is then adjusted to give a net $\frac{\Delta K}{K}$ acceptable to the experimenter. From (6), one requires a maximum acceptance in θ of $\Delta\theta \simeq 10^{-4}$ radian to insure an acceptance in K of $\lesssim 1\%$. This indicates the necessity of accurate angular alignment of the beam and, together with knowledge of the annihilation cross section, serves to define the positron intensity that is required to produce a useful flux of photons in a small solid angle.

When $\theta \ll 1$ and $E \gg M$ the two photon differential annihilation cross section is given by[1]

$$\frac{d\sigma}{d\Omega} = \frac{r_0^2}{2}\,\frac{1}{\left[1+\frac{1}{2}\gamma\theta^2\right]^2}\left(\frac{2}{\gamma\theta^2} + \frac{\gamma\theta^2}{2}\right) \tag{8}$$

where $\gamma = E/M$ and $r_0^2 = 7.95 \times 10^{-26}$ cm^2. Using (5) this can be translated into

$$\frac{d\sigma}{d\Omega} = \frac{r_0^2}{2}\,\frac{\frac{K}{E}\left[\left(\frac{K}{E}\right)^2 + \left(1-\frac{K}{E}\right)^2\right]}{\left(1-\frac{K}{E}\right)} = 2 \times 10^{-26}\ \text{cm}^2\ \text{sr}^{-1}\ ,$$

the last equality applicable for K/E = 1/2. For a solid angle of 10^{-7} ster. and a 15 cm. liquid hydrogen target, this yields 10^{-9} monochromatic photons per incident positron. With the presently available SLAC positron intensity one can thus obtain about 4×10^3 photons per second in this well-defined beam.

The usable photon intensity depends critically upon the tolerable spread in K. Multiple scattering of the positrons in the annihilation target contributes to the spread through (6) and if one chooses a target length to match the contributions to ΔK from the multiple scattering and from the angular acceptance then it is easy to show[2] that the usable intensity varies as the cube of $\Delta K/K$.

Tables of Bremsstrahlung and annihilation cross sections have been calculated[3] as a function of K, E, and θ. Some of the results are shown graphically in Fig. 1. These graphs and Eq. 8 enable one to calculate the monochromatic yield and the Bremsstrahlung "background" for any beam configuration, and show that the optimum ratio of annihilation to Bremsstrahlung radiation is obtained for photon production angles near the "symmetry" point.[4]

III. BEAM CONFIGURATION

The SLAC positron beam[5] exits the linear accelerator, is momentum-analyzed in the beam switchyard and enters the End Station B experimental area. The positron beam is produced by showering an electron beam in a thick target located in the linac at a distance of 2/3 mile from the injector; positrons emitted from the radiator are then accelerated in the remaining 4/3 mile of linac. Reliable positron operation at a maximum energy of 12 BeV can now be achieved at SLAC. Two modes of positron operation are available: (1) A stationary radiator in the linac from which one can derive pulses up to a maximum rate of 360 p.p.s. or, (2) a pulsed targeting arrangement whereby on can attain up to 3 p.p.s. of positrons. The latter mode of

operation is particularly well suited to bubble chamber operation, the remaining electron pulses that are not converted being available for the execution of other experiments.

Figure 2 shows the beam layout. Before striking the liquid hydrogen annihilation target the positrons pass through a small dipole magnet, D1, (not shown) which enables one to impart a small horizontal (~1 mr.) angle to the beam and thus vary the energy of the photons which are transmitted through the collimating system. The primary positron beam is bent vertically downward by the dipole D2 and dumped in a shielded area. The photons emanating from the target are then incident on the first set of horizontal collimators, C1, which serve to define the angular acceptance of the beam. (Two collimators at C1 are shown in Fig. 2; this allowed us to define a photon beam and its complement for the initial tune-up studies.) The collimators are remotely adjustable in position and opening and can be outfitted with different defining surfaces. It is clear that photons of energy K are emitted from the target in a cone of half-angle $\theta(K)$; depending upon the demands of the experiment, the collimation surfaces can be either conical sections or plane. The vertical collimation is done in the vicinity of C1 and it is the vertical acceptance that usually dictates whether one wants to use a curved C1 or approximate that with a plane C1.

The photons transmitted by C1 are then incident on a LiH beam hardener located in dipole D3. Radiation lengths of 1/3, 2/3, or 1 are available. The function of D3 is to sweep out charged background particles and the electron pairs produced in the LiH. The immediate deflection of the pairs in the LiH minimizes the "second-order" Bremsstrahlung that they could contribute to the photon beam. The photon beam then exits the End Station B and is passed through a second collimator C2 which serves to reduce the halo originating from the jaws of C1. A final dipole D4 sweeps the beam of charged particles produced in C2. The definition of the beam is now completed, and the particular experiments may be constructed around it.

Although most experimenters have designed their own distinct photon beam monitors, signals proportional to the positron intensity are available to all; in addition, a scintillation screen located in the positron dump is available for monitoring the positron beam cross section which can be controlled by adjusting the quadrupole focusing magnets in the beam switchyard. The direction and position of the positron beam incident upon the hydrogen radiator can be monitored by two torroid position monitors, one directly before the radiator and one ~30 m. upstream. The positions at these stations may be kept constant to ~2 mm.

IV. INITIAL BEAM MEASUREMENTS

Positrons of 10.2 (±0.5%) BeV were focussed on a 5 cm. liquid hydrogen target. A beam hardener of 2/3 radiation length was used. A small plastic scintillator (6.35 mm wide) with a Pb facing was positioned at a surveyed point (about 28 m from the target), such that it served to define an angle of 10 mrad relative to the positron beam. C1, with a 3.175 mm opening, was traversed horizontally and the counts in the scintillator R2 were recorded normalized to the e^+ torroid intensity monitor. Results are shown in Fig. 3a. From this measurement one can deduce that the positron beam size was less than 3 mm.horizontally. Such a measurement also serves to check the alignment of C1, and similarly C2 may be set to intercept the "wings" of the photon beam.

A second scintillator L2, identical to and in logical coincidence with R2, was then traversed across the spatial region containing the photon beam which was complementary to that striking R2. The resulting coincidence distribution is shown in Fig. 3b. The center of this distribution can be determined to an accuracy of less than 1 mm. This measurement provides a check on the positron energy which, for near symmetrical annihilation, depends only on the opening angle between the two photons.

To obtain a quick on-line measurement of the photon energy spectrum, we used a total absorption shower counter consisting of 16 radiation lengths of Pb sandwiched between 16 pieces of plastic scintillator each of dimension 1/4" × 4" × 4". The counter was placed at the symmetry angle for 10.2 BeV positrons. The pulse-height spectrum is shown in Fig. 4. The width of the distribution is dominated by the counter resolution. The ratio of Bremsstrahlung to annihilation is consistent with the predictions.[2,3]

V. USE OF BEAM IN PHOTOPRODUCTION

To date the annihilation photon beam has been used in two experiments: (1) photoproduction of pion pairs and (2) a study of γp interactions in the SLAC 40" hydrogen bubble chamber.

1. Pion Pair Photoproduction Spark Chamber Experiment

A. Energy Spectrum

The pion-pair photoproduction experiment utilizes a large aperture magnet for momentum analysis of the $\pi^{\pm}$ followed by a system of wire spark chambers which is triggered by some scintillation counters. The entire set up is readily converted into a pair spectrometer which provides a means of measuring the photon beam energy spectrum.

We made measurements on 5 BeV photons from 6.3 BeV positrons, 7 BeV photons from 10 BeV positrons and 9 BeV photons from 12 BeV positrons. We report here the measurements of the 9 BeV photon beam; the lower energy spectra are shown in the next section.

The pair spectrometer configuration is shown in Fig. 5. The photon beam had a cross section of 1 cm × 7.5 cm as it passed through the 0.032 radiation length Aℓ converter located at the entrance of the analyzing magnet. The $e^{\pm}$ pairs

passed through a 12.5 kg-m integrated magnetic field and their exit trajectories were recorded by the wire spark chambers (1 mm wire spacing). Data was logged and track momenta calculated with an on-line IBM 1800 computer. The finite geometrical acceptance of the system produces an energy dependent detection efficiency which has been calculated by a Monte Carlo program which includes the effects of the finite photon beam size and multiple scattering in the converter. The calculation assumes an energy independent pair production cross section and a Bethe-Heitler electron energy distribution.[6] Folding the efficiency into the raw data we arrive at the results contained in Fig. 6.

We have compared the data in Fig. 6 with a further Monte Carlo calculated distribution including the following effects: (1) multiple scattering of the positron beam in the annihilation target, (2) the positron beam phase space, (3) the phase space defined by the collimators, (4) multiple scattering in the pair converter, (5) the spatial resolution of the wire chamber spectrometer. The calculation agrees very well with the observed shape and position of the peak. From this we conclude that this monochromatic beam has a central energy of 8.83 ± 0.05 BeV and a half width at half maximum of 0.26 BeV.

B. Photon Flux

The spectrum was fitted to an expression which included contributions from $e^+ + e^-$ and $e^+ + p$ Bremsstrahlung and the annihilation process (with a Gaussian parameterization). The result is that the data in Fig. 6 contain 40% annihilation photons, while one expects[3] to find a 50% annihilation contribution. We believe the most likely source of the difference is from secondary Bremsstrahlung from e^+ scatters at large angles, and showers in the collimators.

Figure 7 displays the dipion energy spectrum obtained from a Be target. The similarity of the photon spectrum (Fig. 6) and the dipion spectrum is obvious

and immediately indicates that quasi-elastic dipion production dominates the interaction.

The photon flux was normally maintained at a level of 50-100 annihilation photons per pulse. This level was dictated by the requirement of reducing spurious sparks in the spark chambers to a tolerable level. The maximum flux available was about 3-4 times greater than that used.

C. Photon Beam Monitors

The photon beam was monitored by converting the last sweeping magnet (D4) into a pair spectrometer. A thin converter was located at C2 and two 2" × 2" scintillators positioned symmetrically at the exit of D4. The coincidence rate was maximized by varying the magnetic field in D4 for each monochromatic energy used. The response was qualitatively similar to results in Fig. 6. This method provides an energy sensitive on-line monitor with minimal interference with the beam.

A second on-line monitor (for checking the D4 pair spectrometer stability) consisted of a scintillator located in a block of tungsten in which we dumped the transmitted photons. The output current of this counter was integrated and recorded on a digital voltmeter which was periodically interrogated by the computer.

2. Photoproduction Experiment In The Hydrogen Bubble Chamber

The SLAC 40" hydrogen bubble chamber has been exposed to the annihilation beam and over one million photographs taken. The chamber is cylindrical, has a visible diameter of 40" at the central plane of the chamber and has a depth of 20". The illumination is the bright field type, using a "Scotch-lite" surface on the face of the piston expander. The chamber has a central magnetic field of 26 KG, varying by less than 4% over the volume of the chamber.

In order to achieve ±1.5% energy resolution, so that the beam energy error will be smaller than the average charged track measurement error in the bubble

chamber, the target length used was 15 cm. This introduces an average photon energy spread of around ±1% for 8-12 GeV positrons with an approximately equal contribution from positron energy and angular spread. Since the position of the photon interaction in the bubble chamber is determined to ± 0.5 mm by geometrical reconstruction, the uncertainty in production angle is not determined by the photon beam collimators but rather by the uncertainty due to positron displacement and angle at the hydrogen radiator. Therefore the photon beam collimators could be opened to allow a convenient flux of photons in the chamber. The resulting beam spectrum in the chamber therefore contained a range of photon energies with each interaction assigned an incident energy within an uncertainty of order ~± 100 MeV, sufficient to identify the reactions by kinematic fits.

The exposures were taken at photon energies between 4 and 8 GeV with the beam parameters shown in Table I. For these exposures the jaws of collimators C_1 and C_2 were curved. The C_1 jaws had a 13" thickness of lead in the beam direction while the C_2 jaws had a 4" thickness of tungsten. The resulting photon beam at the position of the bubble chamber (60 m.from the H_2 radiator) was about 50×5 cm^2 in area. One radiation length of LiH was inserted at D3 as beam hardener. With these settings the average annihilation photon flux was ~50 annihilation photons per picture.

The spectrum of pair energies obtained by measuring all pairs of energy greater than 100 MeV is shown in Fig. 8, for the 5.2 BeV exposure. The resolution obtained by calculating the production angle from the position of the interaction in the bubble chamber is shown in Fig. 9. Here the number of photons is plotted against the difference between measured and calculated pair energy. The width of the approximately gaussian peak around zero difference is ± 2.5%, which is compatible with the estimated true photon energy spread and the track measurement

errors (the latter spread is abnormally large owing to Bremsstrahlung energy loss of the electrons and the positrons in the chamber).

Using the photon energy constraint, it has been shown that a clean separation of events with a single neutral particle from those with zero neutrals and with more than one neutral particle is obtained.[8]

Table I

Bubble Chamber Exposure Conditions			
Mean Photon Energy BeV	Positron Energy BeV	Production Angle mrad	Number of Photographs
4.25	8.5	10.95	330 K
5.2	10.0	9.6	360 K
7.5	12.0	7.15	620 K

ACKNOWLEDGEMENTS

The construction and testing of the annihilation beam involved many people whose contribution was vital. We would like to thank in particular H. De Staebler, J. Pine, G. Loew, R. Miller and J. Voss for the positron source, J. Harris, A. Baumgarten, F. Halbo, R. Friday, L. Johnson, J. Faust, the Research Area Division and Electronics groups for construction and instrumentation, L. Kaufmann, V. Perez-Mendez and A. Stetz for the wire spark chamber system, W. B. Johnson, R. Giese, M. Beniston, R. Russell, A. Levy, T. H. Tan, E. Pickup, P. Klein and G. Wolf for help during runs, and R. Watt, R. Blumberg, J. Mark, J. Alcorn, S. St. Lorant, B. Sukiennicki, H. Barney for design and operation of the chamber. In addition we thank the scanning and computation groups for data reductions.

FIGURE CAPTIONS

1. Calculated ratios of Bremsstrahlung to annihilation radiation yields for various values of positron energy E+ and accepted photon energy $E\gamma$.
2. Conceptual schematic of annihilation beam.
3a. Photon intensity rate at a fixed position of scintillator R2 as collimator C1 is traversed across the beam line with a fixed 1/8" opening.
3b. Coincidence rate between counters R2 and L2 when R2 position is fixed and L2 is traversed across the complementary beam line. See Section III.
4. Photon energy spectrum observed with a total absorption counter placed at an angle of 10 mr relative to a 10.2 BeV positron beam.
5. Arrangement of experimental apparatus into a pair spectrometer for spectrum measurements.
6. Results of measurement of photon spectrum with pair spectrometer. The solid curve shows the shape expected for a photon beam of 0.26 BeV HWHM and the energy dependent acceptance and detector resolution folded in.
7. Energy spectrum of pion pairs from one reaction $\gamma + \text{Be} \rightarrow \pi^+ + \pi^- + \text{Be}$, using the annihilation beam set up for 9 BeV photons.
8. Pair energy spectrum measured in the 40" hydrogen bubble chamber for the 5.2 BeV photon energy run.
9. Number of pairs versus the difference between measured pair energy and that calculated from the vertex position in the chamber.

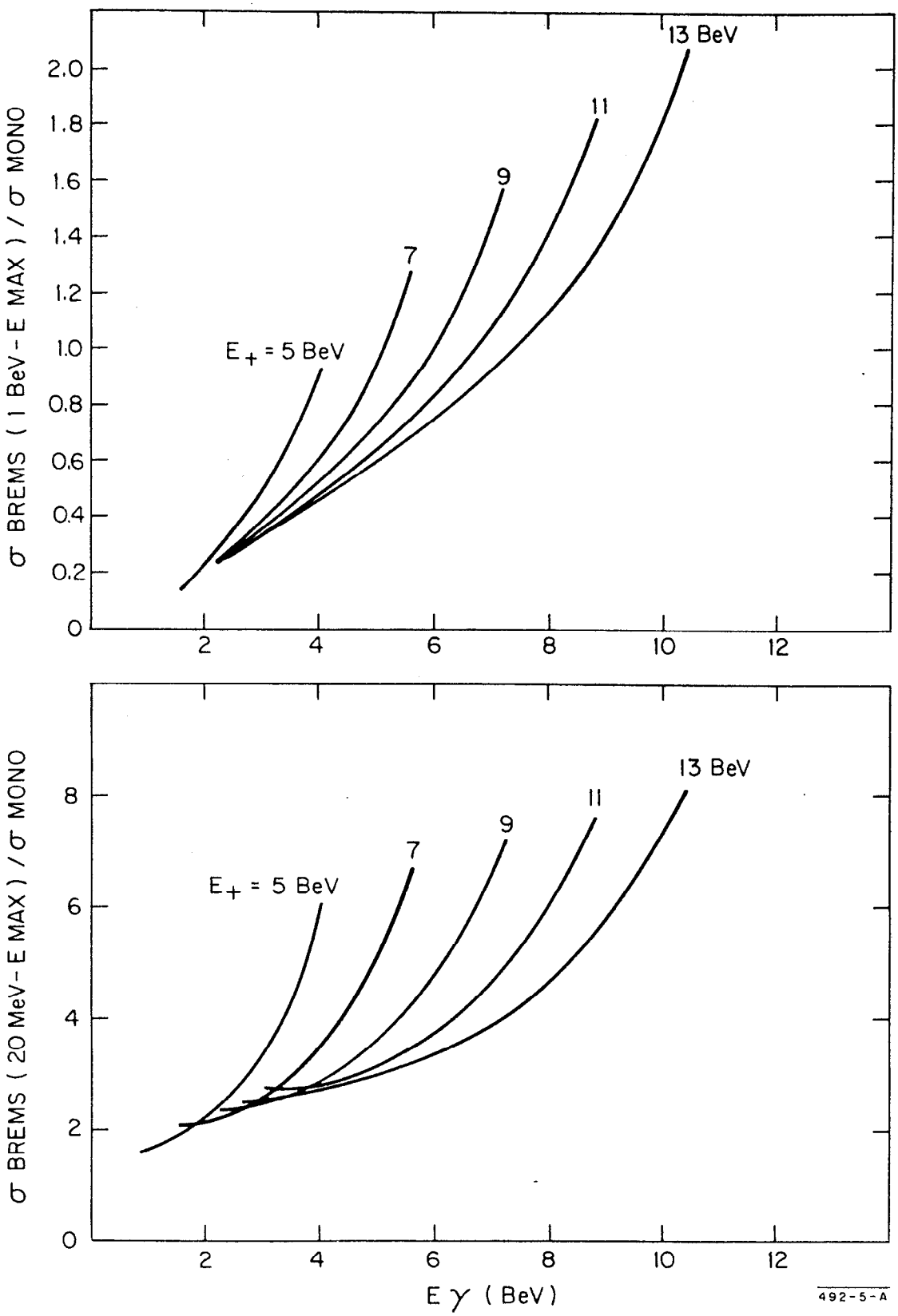
σ BREMS (1 BeV - E MAX) / σ MONO
2.0
1.8
1.6
1.4
1.2
1.0
0.8
0.6
0.4
0.2
0
2
4
6
8
10
12
13 BeV
11
9
7
E+ = 5 BeV
σ BREMS (20 MeV - E MAX) / σ MONO
8
6
4
2
0
2
4
6
8
10
12
13 BeV
11
9
7
E+ = 5 BeV
E γ (BeV)
492-5-A

Fig. 1

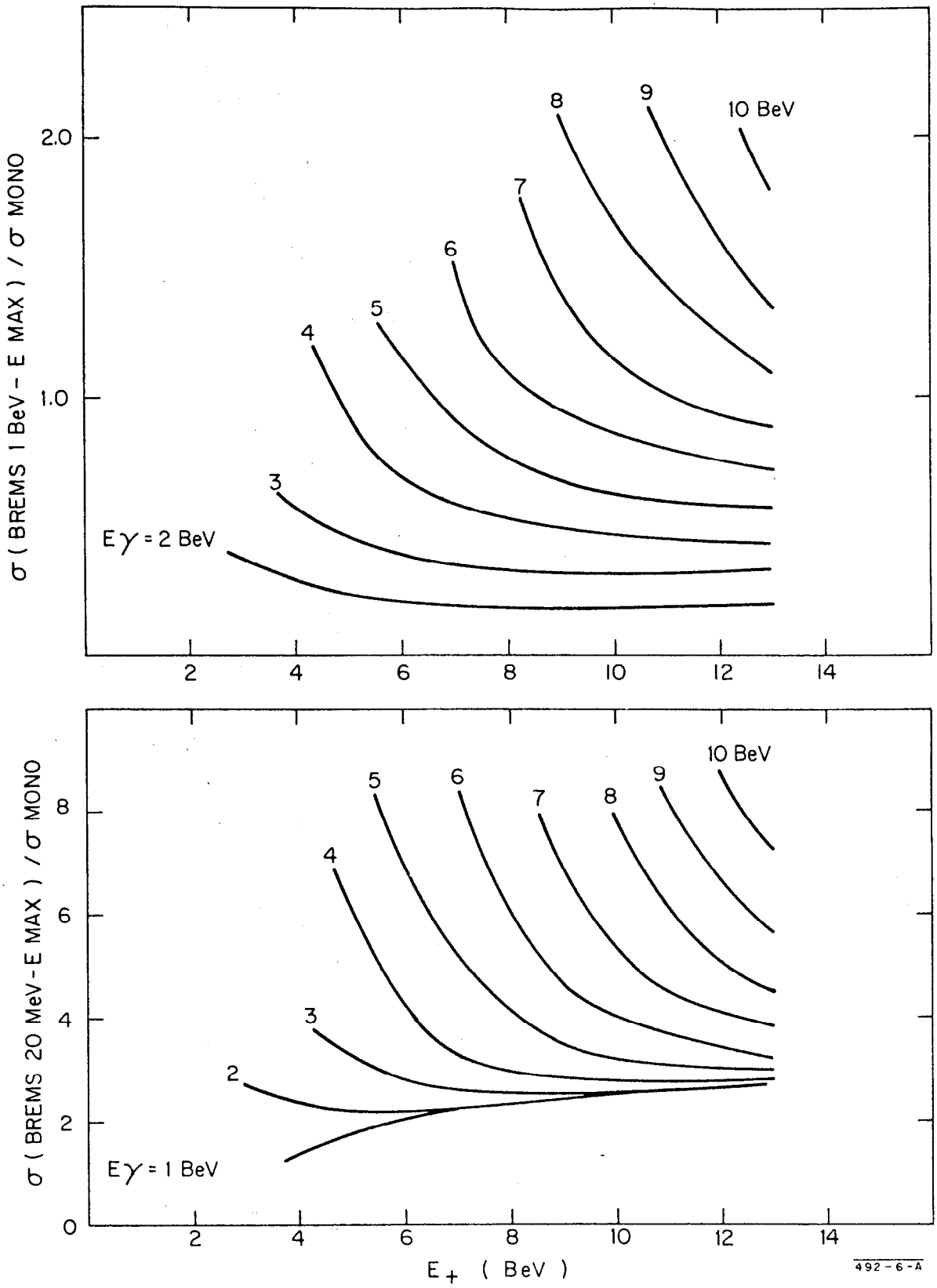
σ (BREMS 1 BeV - E MAX) / σ MONO
2.0
1.0
2
4
6
8
10
12
14
10 BeV
9
8
7
6
5
4
3
Eγ = 2 BeV
σ (BREMS 20 MeV - E MAX) / σ MONO
0
2
4
6
8
10
12
14
10 BeV
9
8
7
6
5
4
3
2
Eγ = 1 BeV
E+ (BeV)
492-6-A

Fig. 1

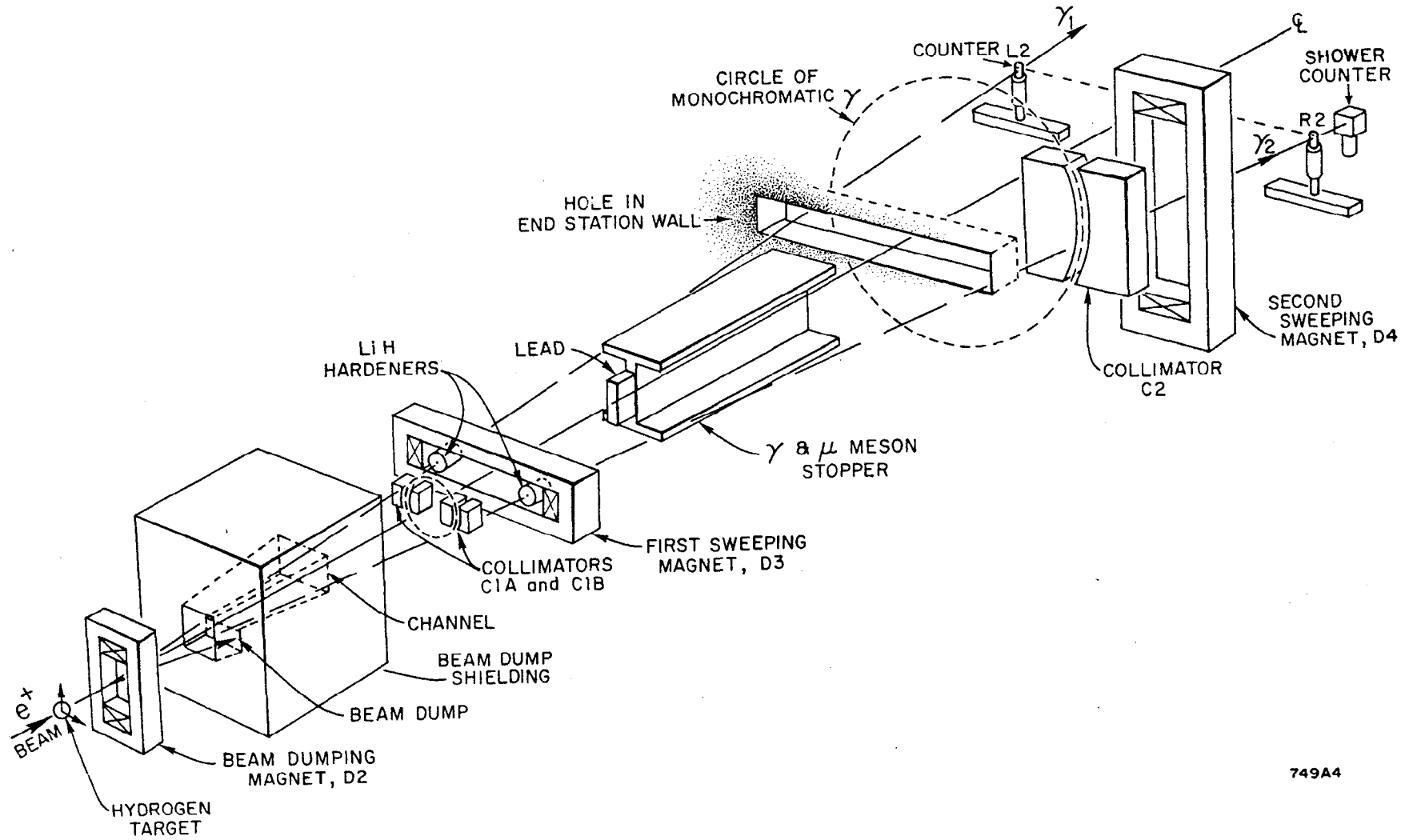
γ_1
COUNTER L2
CIRCLE OF MONOCHROMATIC γ
HOLE IN END STATION WALL
SHOWER COUNTER
R2
γ_2
SECOND SWEEPING MAGNET, D4
COLLIMATOR C2
LiH HARDENERS
LEAD
γ & μ MESON STOPPER
FIRST SWEEPING MAGNET, D3
COLLIMATORS C1A and C1B
CHANNEL
BEAM DUMP SHIELDING
BEAM DUMP
BEAM DUMPING MAGNET, D2
HYDROGEN TARGET
e+ BEAM
749A4

Fig. 2

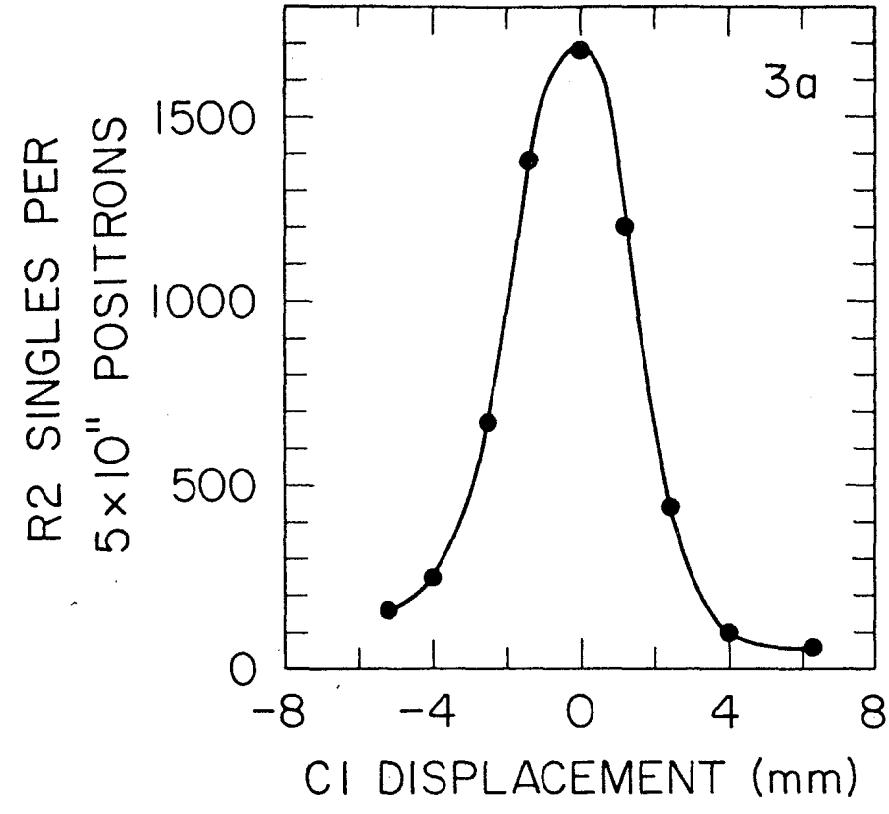
3a
R2 SINGLES PER
5×10" POSITRONS
1500
1000
500
0
-8
-4
0
4
8
C1 DISPLACEMENT (mm)

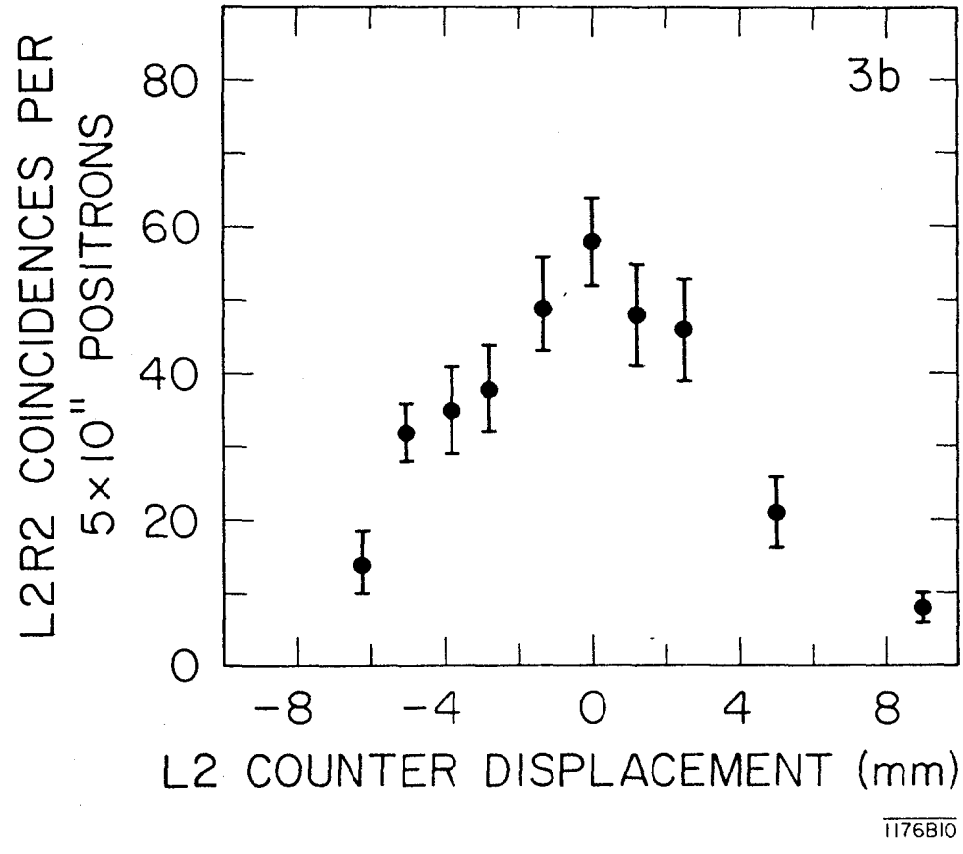
3b
L2R2 COINCIDENCES PER
5×10" POSITRONS
80
60
40
20
0
-8
-4
0
4
8
L2 COUNTER DISPLACEMENT (mm)

1176810

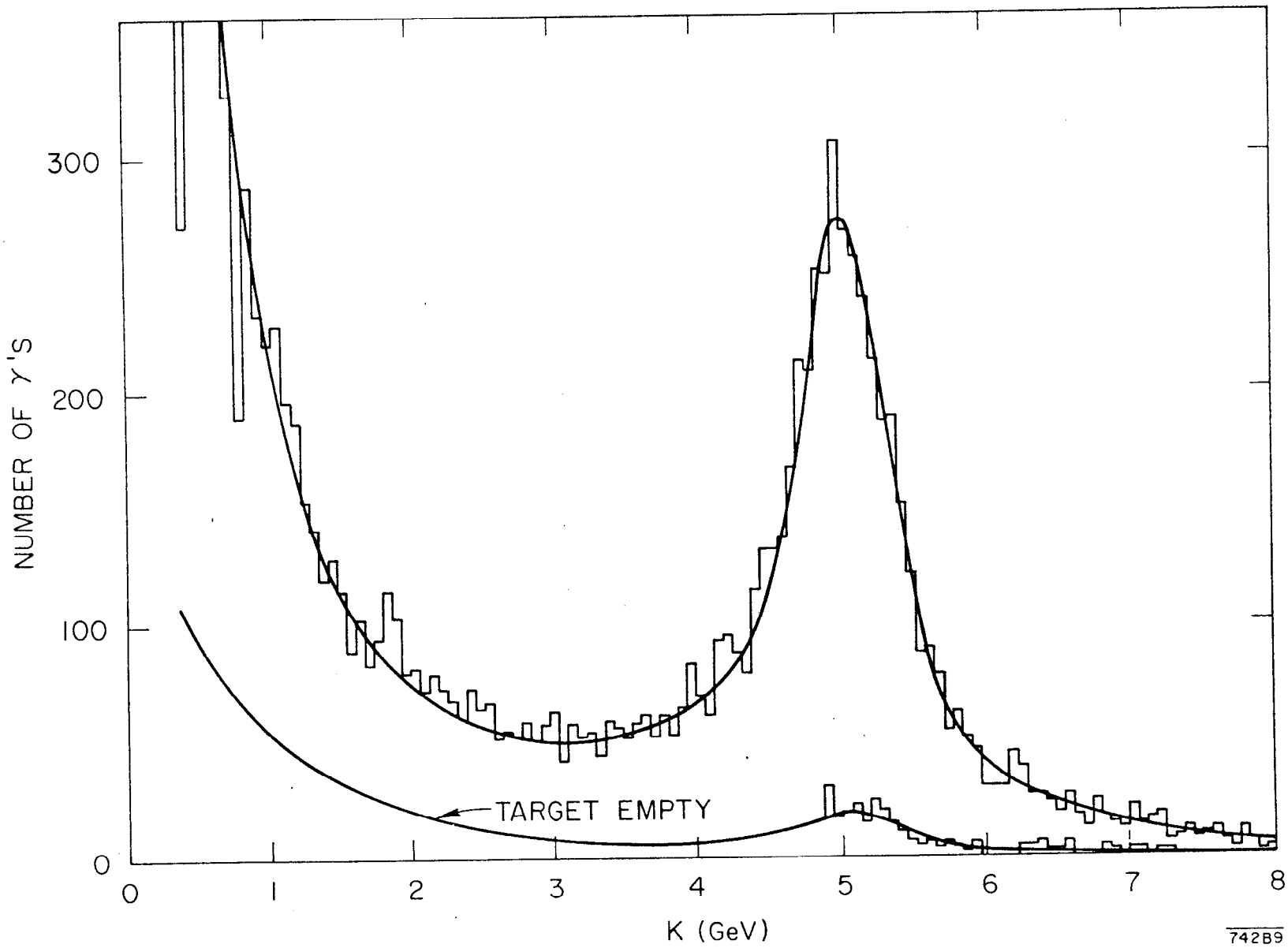

Fig. 4

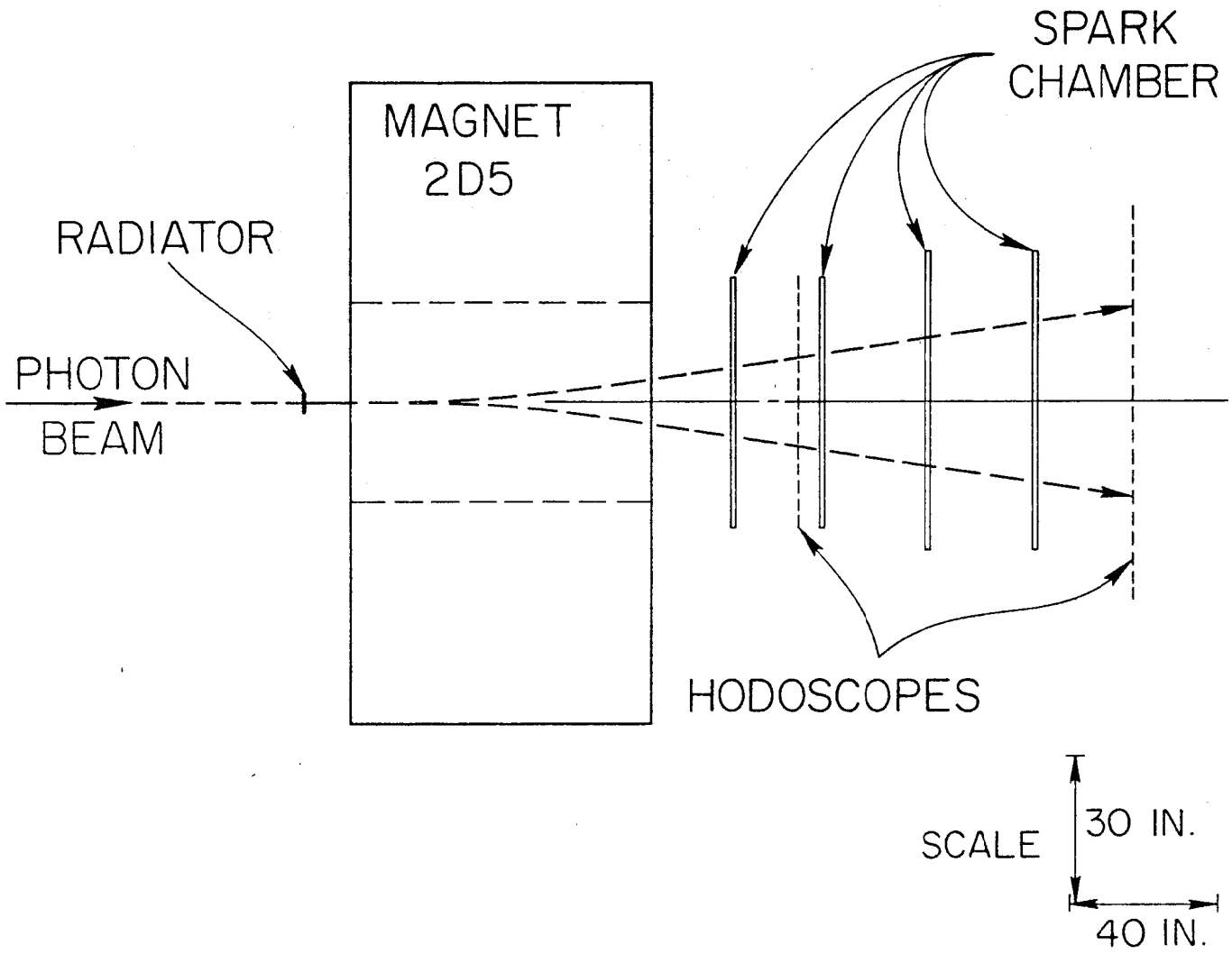
SPARK
CHAMBER
MAGNET
2D5
RADIATOR
PHOTON
BEAM
HODOSCOPES
SCALE
30 IN.
40 IN.
1176A9

Fig. 5

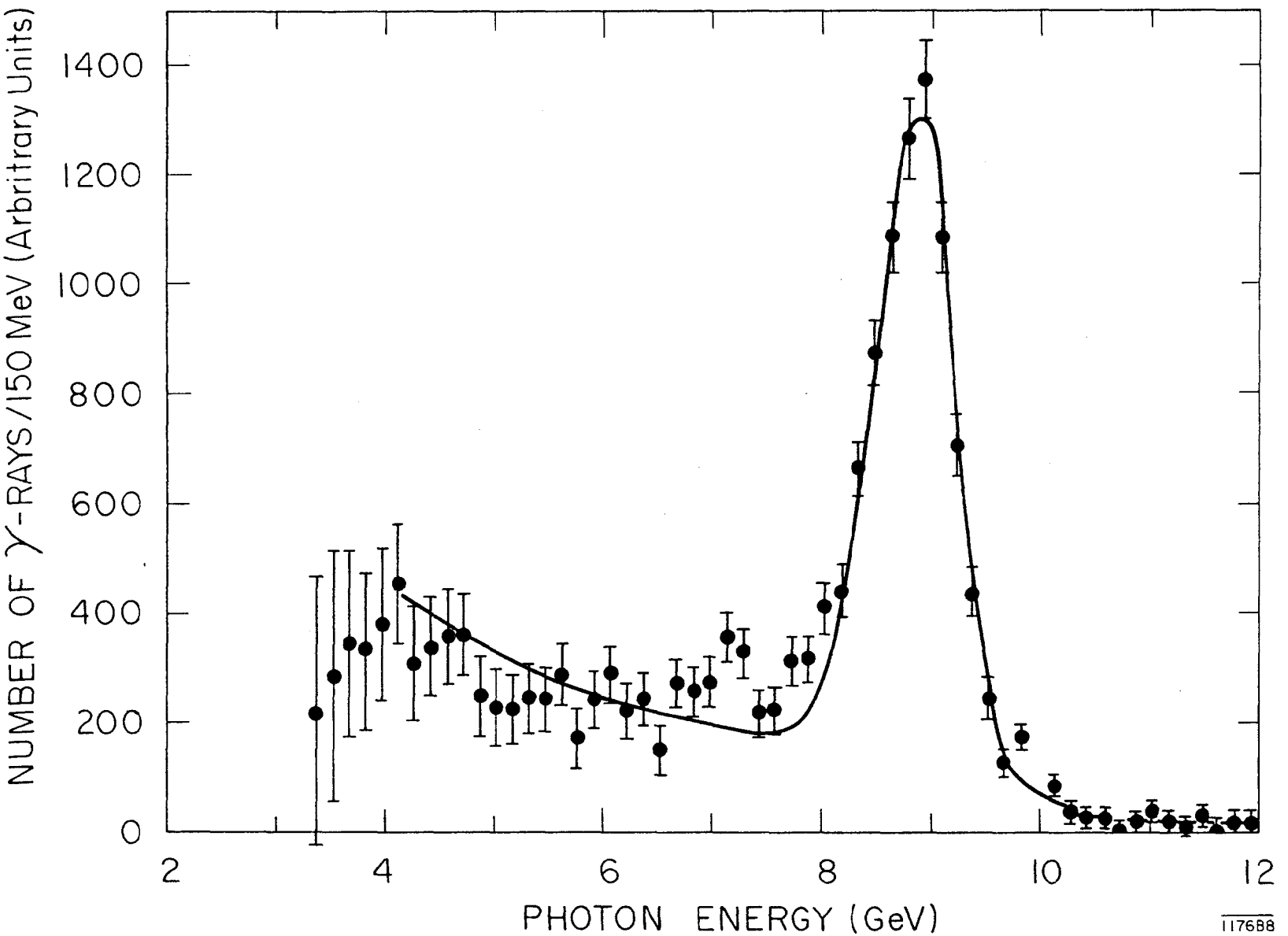
NUMBER OF γ-RAYS/150 MeV (Arbitrary Units)
0
200
400
600
800
1000
1200
1400
2
4
6
8
10
12
PHOTON ENERGY (GeV)
117688

Fig. 6

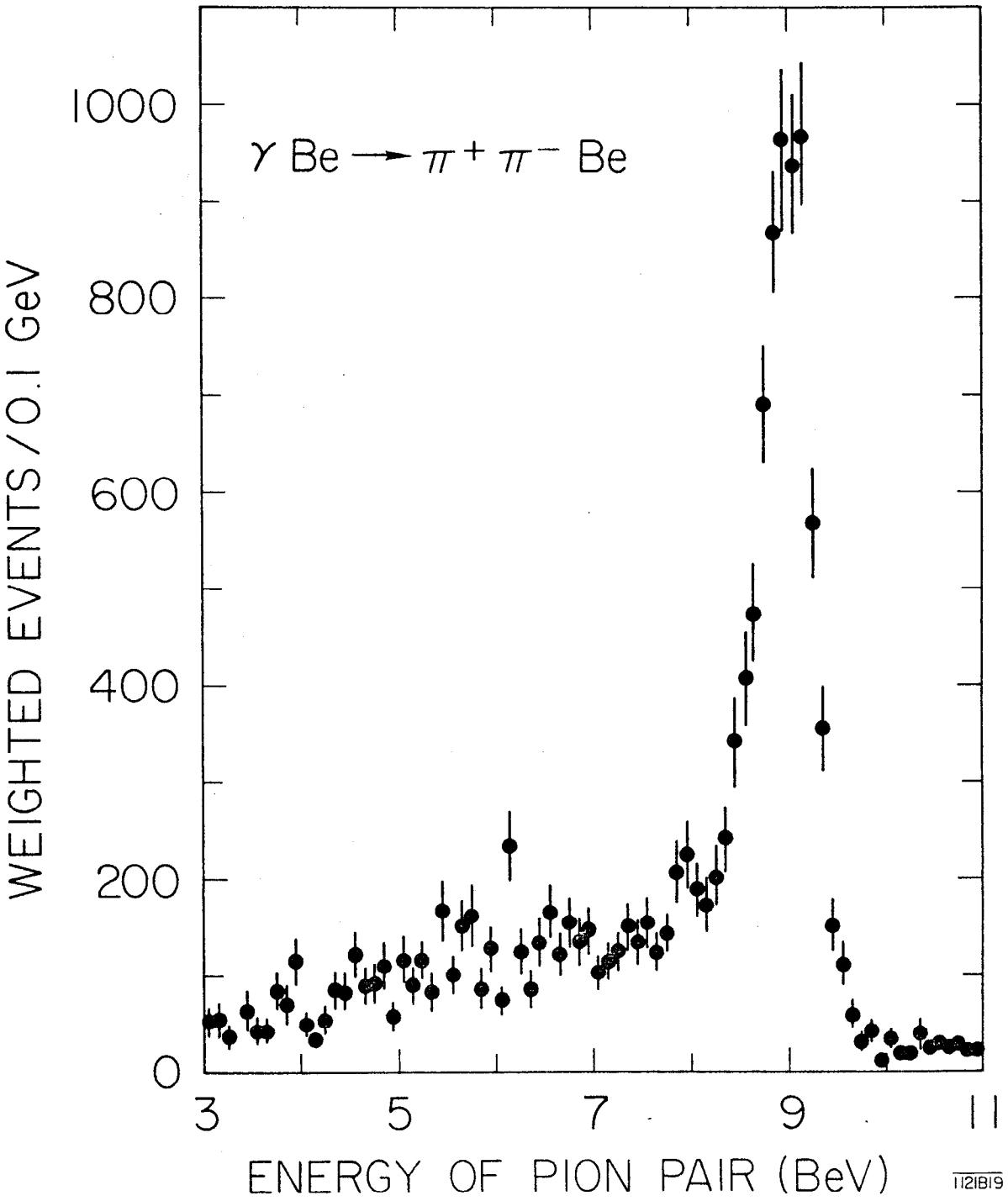
1000
800
600
400
200
0
WEIGHTED EVENTS / 0.1 GeV
γ Be → π+ π− Be
3
5
7
9
11
ENERGY OF PION PAIR (BeV)
1121B19

Fig. 7

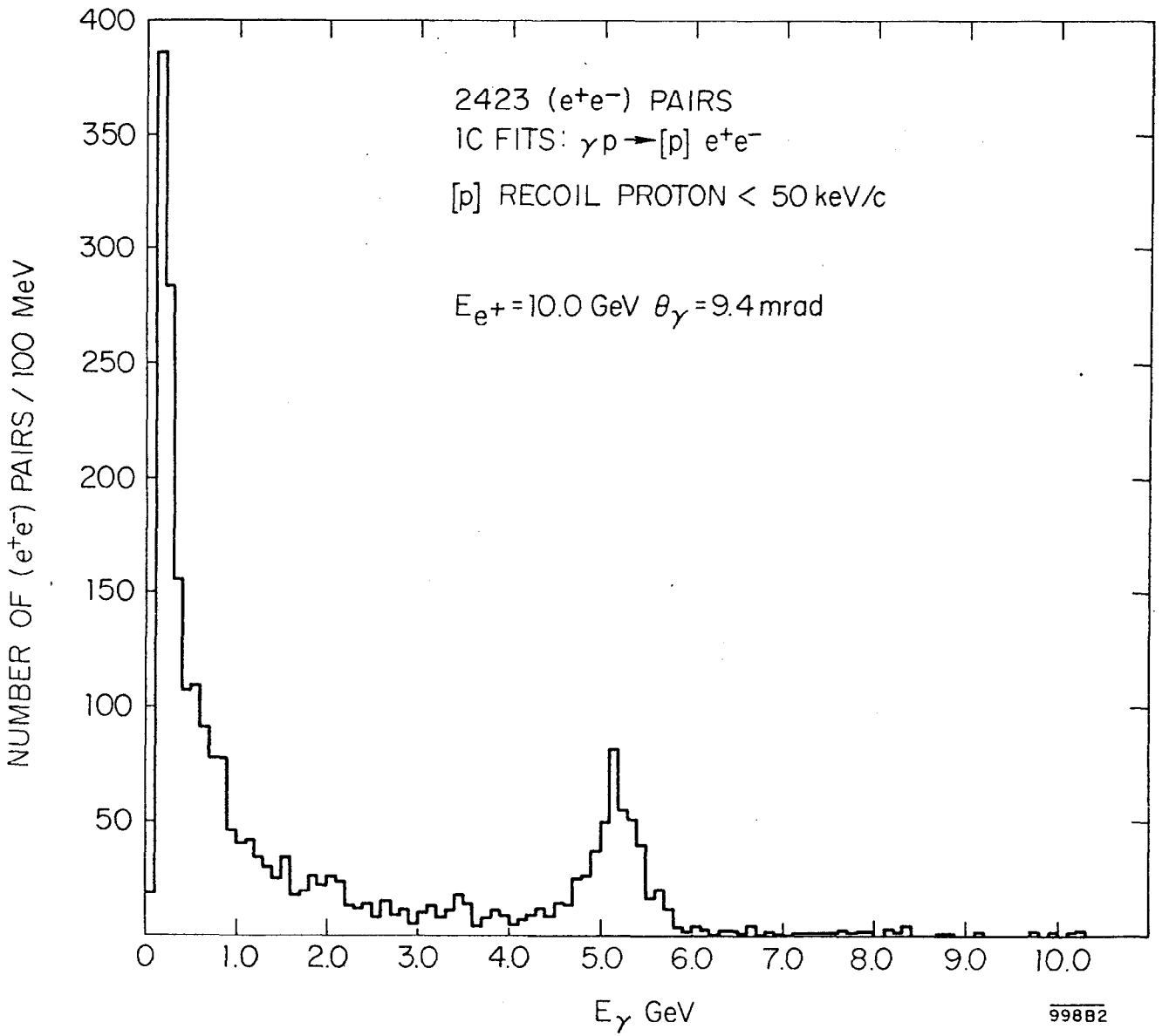
2423 (e+e−) PAIRS
1C FITS: γp → [p] e+e−
[p] RECOIL PROTON < 50 keV/c
Ee+ = 10.0 GeV θγ = 9.4 mrad
NUMBER OF (e+e−) PAIRS / 100 MeV
400
350
300
250
200
150
100
50
0
1.0
2.0
3.0
4.0
5.0
6.0
7.0
8.0
9.0
10.0
Eγ GeV
998B2

Fig. 8

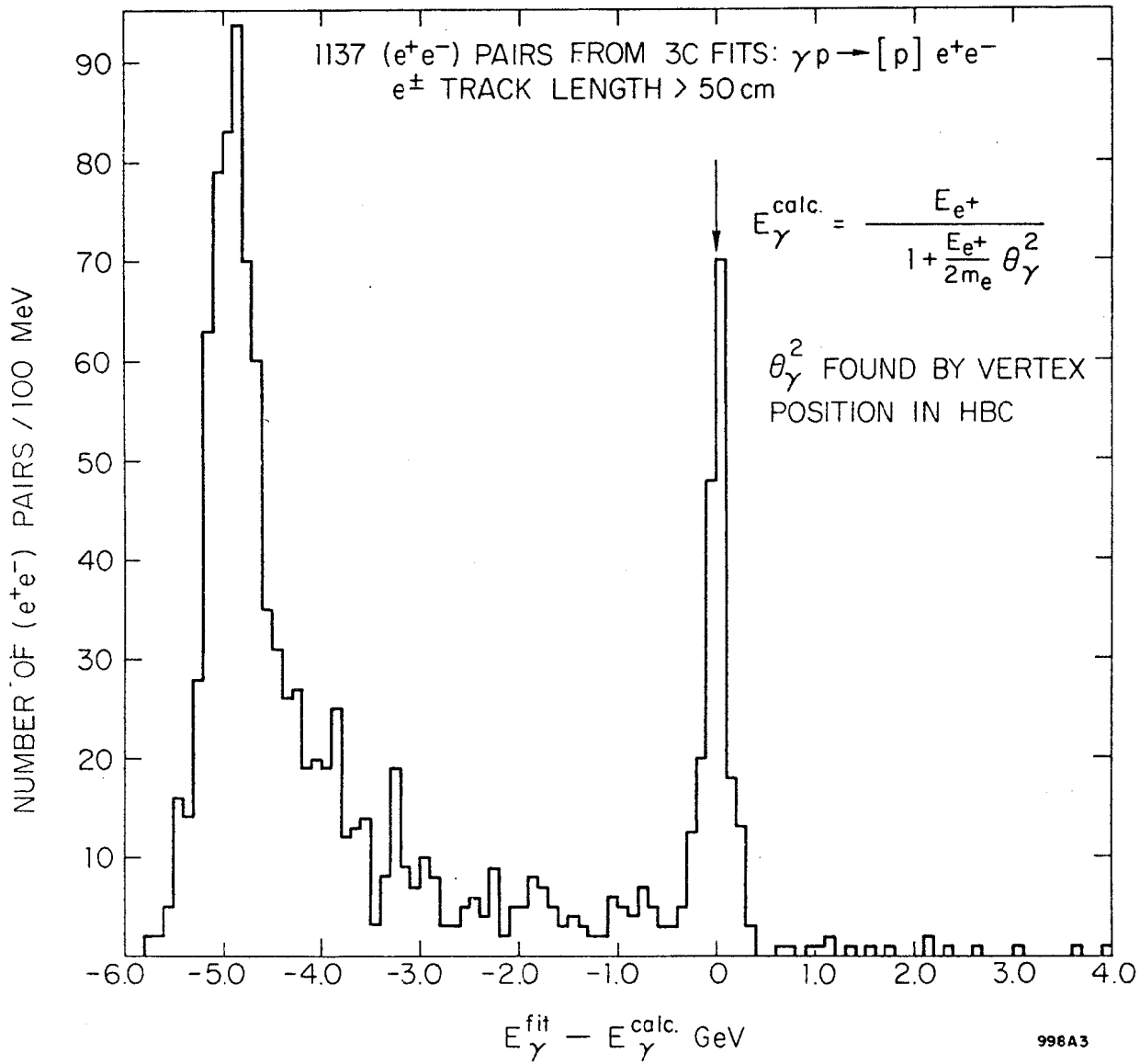
1137 (e^+e^-) PAIRS FROM 3C FITS: $\gamma p \rightarrow [p]\, e^+e^-$
$e^\pm$ TRACK LENGTH > 50 cm
$E_\gamma^{calc.} = \frac{E_{e^+}}{1+\frac{E_{e^+}}{2m_e}\theta_\gamma^2}$
θ_γ^2 FOUND BY VERTEX POSITION IN HBC
NUMBER OF (e^+e^-) PAIRS / 100 MeV
90
80
70
60
50
40
30
20
10
-6.0
-5.0
-4.0
-3.0
-2.0
-1.0
0
1.0
2.0
3.0
4.0
$E_\gamma^{fit} - E_\gamma^{calc.}$ GeV
998A3

Fig. 9